

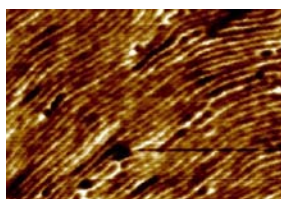
## Elite Study Program "Macromolecular Science"

### Module IP - Interdisciplinary Practical Course: *"Amphiphilic block copolymers as a model system for drug delivery"*

#### *Macromolecular Chemistry*



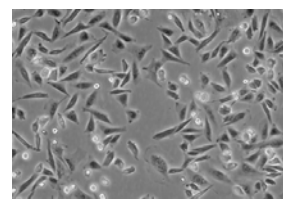
#### *Physical Chemistry*



#### *Experimental Physics*



#### *Process Biotechnology*



**Professors of the University of Bayreuth**

**Prof. Dr. Mukundan Thelakkat**

**Dr. Andreas Bernet (Coordination)**

**Summer Term 2015**

## **i. Introduction**

This teaching module comprises an actual interdisciplinary practical course conducted in a team of two students. Its aim is to gain practical knowledge about an application of micelle-forming amphiphilic diblock copolymers as an example of a model drug delivery system.

Four sets of experiments will be conducted by the students. The overview of experiments is presented in Part 3.

Four research assistants will help the students in conducting the experiments. For further questions please contact Dr. Andreas Bernet ([enb.macromolecularscience@uni-bayreuth.de](mailto:enb.macromolecularscience@uni-bayreuth.de)).

## **ii. Motivation**

Amphiphilic diblock copolymers, e.g. poly(ethylene oxide)-*block*-poly(*n*-butyl acrylate) (PEO-PnBA), consist of a hydrophilic and a hydrophobic polymeric block covalently attached to each other. In a solvent, which is selective for the hydrophilic block, e.g. water, they form micelles above the critical micellar concentration (cmc). These micelles are aggregates of polymer chains, where the hydrophobic parts are collapsed and form the core, whereas the hydrophilic parts form the corona or shell. There are two different types of spherical micelles: star type micelles with a thin core and a thick corona, and “crew-cut” micelles with a thin (or “crew-cut”) corona and a thick core. Depending on the composition one can also find wormlike or cylindrical micelles. Diblock copolymers usually have a lower cmc than low molecular weight surfactants.

Vesicles or other aggregates may also be formed by this procedure. A vesicle is a spherical hollow (filled with solvent) aggregate, which is formed by a spherical shell consisting of a (in some cases multi-) double-layer of the amphiphilic block copolymers.

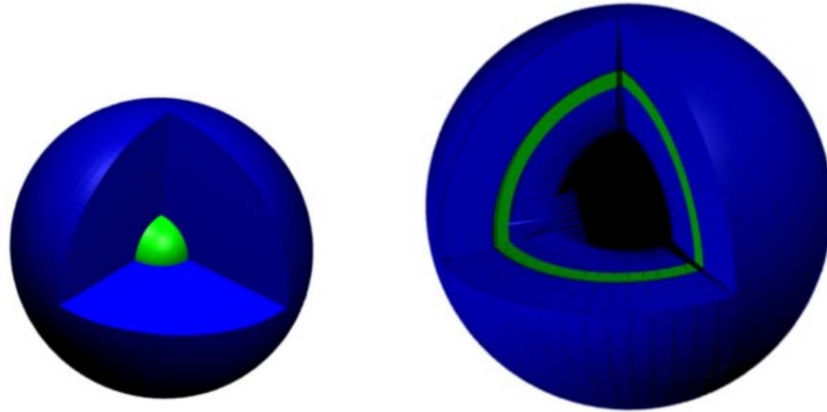


**Figure I** Left: spherical star micelle. Right: vesicle. Green and blue depict the blocks of different polarity.

Adapted from <http://arxiv.org/ftp/cond-mat/papers/0503/0503084.pdf>.

Applications of the diblock copolymer solutions comprise drug delivery, imaging, sensorics, usage as agents for emulsion polymerization, stabilization of dispersions and biomimetic chemistry.

For the application as drug delivery systems the hydrophilic block is chosen to be biocompatible and the hydrophobic part of the micelles forms a reservoir for a more hydrophobic drug. The micelles are taken up by the target cells by endocytosis and can release their content over a long time period or following a stimulus, such as temperature, pH, ionic strength or light. The usual retention is longer compared to low molecular weight surfactants.

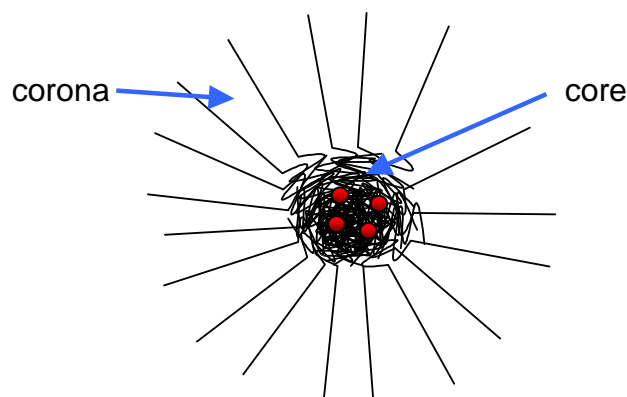


**Figure II** Micelle loaded with a fluorescent label (red) as model for a micelle loaded with a hydrophobic drug.

Such drug delivery systems are characterized by a high drug loading capacity and a narrow size distribution. Their size can be tuned to facilitate their uptake by endocytosis. The attainable size range comprises also the size of viruses. When the drug is replaced by an organic fluorophore or an inorganic quantum dots (made from semiconductors) this system can be studied as a model system in imaging using fluorescence microscopy. Targeting can be achieved actively by using receptor-ligand interactions or passively *e.g.* using the so-called Enhanced Permeation and Retention (EPR-) effect of malignant tumours, which are characterized by a defective vascular architecture, fast growth and possibly a marginal expression of the lymphatic system. Of course stimuli-sensitive micelles can also be used as sensors for the respective stimulus.

Like low molecular weight surfactants, the amphiphilic diblock copolymers have also applications as stabilizers of dispersions. They can be used in emulsion polymerization. Emulsion polymerization is a process used to prepare polymeric spheres of controlled size. The solvent for the monomer is dispersed in a second solvent, in which the monomer is not soluble and which is not miscible with the first solvent. The size of the droplets thereby formed can be controlled by the ratio of surfactant and solvents used.

Other important applications of block copolymers in the solid state include holographic data storage, photovoltaics, surface modification, blending agents to improve the mechanical stability of thin films, and molecular electronics.

### iii. Overview of Experiments, Responsible Chairs and Assistants

I) The diblock copolymer will be characterized by **Proton Nuclear Magnetic Resonance** ( $^1\text{H-NMR}$ ) and by **Size Exclusion Chromatography** (SEC). For comparison purposes poly-n-butyl acrylate (PnBuA) will be synthesized by **Free Radical Polymerization**. **(1 day)**

Macromolecular Chemistry I, Prof. Dr. H.-W. Schmidt;

Dr. Andreas Bernet, [andreas.bernet@uni-bayreuth.de](mailto:andreas.bernet@uni-bayreuth.de), Phone: 3298, MCI

II) Micelles of the diblock copolymer which are loaded with an organic fluorophore, will be characterized using **Fluorescence Correlation Spectroscopy** (FCS). **(1 day)**

Experimental Physics IV, Prof. Dr. J. Köhler.

Dr. Martti Pärs, [Martti.Paers@uni-bayreuth.de](mailto:Martti.Paers@uni-bayreuth.de), Phone: 4003, EPIV

III) Thin films and micelles of the diblock copolymer will be investigated by **Atomic Force Microscopy** (AFM, also called SFM, Scanning Force Microscopy). **(1 day)**

Physical Chemistry II, Prof. Dr. A. Fery.

Dr. Daria Andreeva-Bäumler, [daria.andreeva@uni-bayreuth.de](mailto:daria.andreeva@uni-bayreuth.de), Phone: 3932, PCII

IV) The micelles will be investigated as a drug delivery system on living mammalian cells, using the organic fluorophore as a model for the drug. **Flow Cytometry** and **Fluorescence Microscopy** (optional) will be applied to provide evidence about the endocytosis of the micelles and the distribution of the micelles in the target cells. **(2 days)**

Process Biotechnology, Prof. Dr. R. Freitag.

Dr. Valerie Jérôme, [valerie.jerome@uni-bayreuth.de](mailto:valerie.jerome@uni-bayreuth.de), Phone: 7372, Process Biotechnology

#### iv. Literature

[1] J. E. Chung, T. Okano; „Thermoresponsive Polymeric Micelles for double targeted drug delivery“ in R. M. Ottenbrite and S. W. Kim (ed.) „Polymeric Drugs & Drug Delivery Systems“, CRC Press, Boca Raton, 2002.

[2] R. Savic, L. Luo, A. Eisenberg, D. Maysinger; „Micellar nanocontainers distribute to defined cytoplasmic organelles“, *Science* **300**, 615-618 (2003).



### Evaluation:

The students will be given the characterization data of the diblock copolymer. This includes data from size exclusion chromatography (SEC, also named gel permeation chromatography, GPC) and from proton nuclear magnetic resonance ( $^1\text{H-NMR}$ ). The students have to evaluate the corresponding block lengths of the EO and nBuA block, respectively, and will calculate the overall molecular weight of the block copolymer using the corresponding  $^1\text{H-NMR}$  data (for an assignment of the proton signals of the block copolymer see Fig. 1.1). Differences between the results calculated from NMR data and from SEC evaluation shall be discussed.

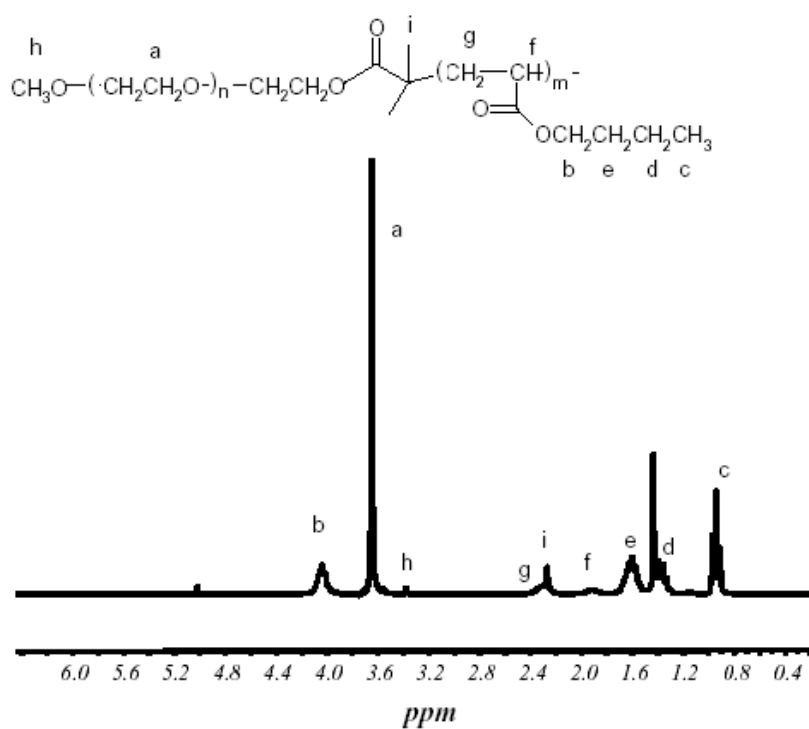


**Figure 1.1.**  $^1\text{H-NMR}$  spectrum (250 MHz) of a PEO-PnBA block copolymer and assignment of the peaks (data from S. Graus Molinero).



## 1.2 Synthesis of Poly(n-butyl acrylate)

### **AIM:**

To show the differences (average molecular weight, molecular weight distribution, polydispersity index (PDI)) between the outcome of controlled radical polymerization and free radical polymerization, the students will prepare a sample of poly(n-butyl acrylate) (PnBuA) by thermally induced free radical polymerization of n-butyl acrylate with azo-bis-isobutyronitrile (AIBN) and compare it with the amphiphilic block copolymer (see 1.1).

### *Preparation of PnBuA by free radical polymerization*

About 10 ml of n-butyl acrylate are dissolved in 30 mL of cyclohexane (p.a.) and filtered through a short column (ca. 3-4 cm filling height) of Alox B (I) (alkaline aluminium oxide) to remove the inhibitor. Ca. 0.05 g of AIBN are added. In order to remove oxygen, the resulting mixture is stirred for 10 minutes while applying an argon stream using a Schlenk flask equipped with a gas tube or *via* a hollow needle and a septum (see Fig. 1.2). Subsequently, a reflux condenser is added while maintaining the argon atmosphere and the flask is put into an oil bath. After stirring at 80 °C for 2 hours, the mixture is allowed to cool down. For SEC experiments about 2-3 mL of the polymer solution are dried under reduced pressure (rotary evaporator, 60 °C, 15 min) yielding a glue-type residue.

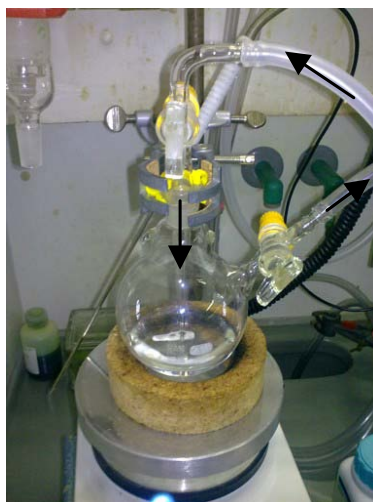


**Figure 1.2:** Removal of oxygen from the monomer solution with argon stream.

*(Poly-) SEC analysis of PnBuA*

About 10 mg of the yielded crude polymer is dissolved in 2-3 ml of THF (from the "Poly"-SEC reservoir). 2 drops of ortho-dichlorobenzene are added as internal standard and the mixture is filtered directly into the sample vial using a 0.2  $\mu\text{m}$  PTFE syringe filter. The vial is sealed with a septum screw cap, labelled ("IHP+IS" and the corresponding date) and submitted to the SEC measurement.

***Evaluation:***

The students will receive the data from the SEC measurements for both the diblock copolymer and the homopolymer (ASCII text files; column 1: molecular weight vs. polystyrene standard; column 2: relative (weighted) intensity of refractive index (RI) detector; column 3: integral). Furthermore, a printout of the SEC traces and the resulting molecular weight distribution will be supplied by the supervisor (*Note:* the "D" value on the printout is the corresponding PDI).

The students have to compare and explain the differences of the molecular weight distribution of the block copolymer and the homopolymer.

*Note:* Additional to a graph where both molecular weight distributions are compared it is recommended to summarize all relevant data ( $M_w$ ,  $M_n$ , PDI) in form of a table.

## **2. Fluorescence Correlation Spectroscopy**

### **2.1. Introduction**

Fluorescence Correlation Spectroscopy (FCS) facilitates the measurement of diffusion constants and concentrations of single molecules, aggregates and particles using smallest amounts of samples. Pre-requisite for these investigations is, that the particles to be investigated fluoresce.

The fluctuations of the detected fluorescence intensity in a small observation volume depend on the diffusion of the fluorophores into and out of the observation volume. The diffusion constant can be determined from the characteristic stay time (or diffusion time) in the known observation volume. As the diffusion constants are linked to the size of the diffusing particle (aggregate, single molecule) applications of FCS can also be found in the detection of the association of ligands and receptors.

In this experiment you will measure the diffusional properties and the concentrations of the labelled nano-particles. The labelling efficiency can be estimated by comparison to the DLS results.

### **2.2. Theory**

Fluorescence Correlation Spectroscopy like dynamic light scattering is a technique which like DLS includes the measurement of a temporal autocorrelation function of a light intensity. Other than in DLS the measured light is incoherent (fluorescence) and therefore only the fluctuations of the number of the nano-particles in the observation volume are correlated. These number fluctuations are caused by the diffusion of the fluorophores into and out of the observation volume, which is given by the excitation with a focused laser beam and by the confocal detection using a small detector.

For the measurements of the diffusive properties of the micelles using fluorescence correlation spectroscopy the set-up is first calibrated using the dye Rhodamine 6G with known diffusion constant from the literature. Afterwards the diffusion of the labelled micelles is measured. Thereby the number-weighted average hydrodynamic radius, and the distribution of the hydrodynamic radii of the block-copolymer micelles can be obtained.

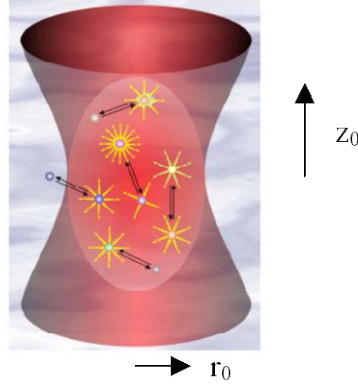


**Figure 2.1.** Confocal Volume and its parameters  $r_0$  and  $z_0$  [P. Schwille and E. Haustein, 2002].

In order to extract the interesting parameters from the measured fluorescence intensity data  $I(t)$  the autocorrelation function  $G(\tau)$  (1) is calculated.

$$G(\tau) = g_2(\tau) = \frac{\langle I(t)I(t + \tau) \rangle}{\langle I(t) \rangle^2} \quad (1)$$

A simplified version of the autocorrelation function for FCS is depicted in Fig. 2.2 and given below.

$$G(\tau) = \frac{1}{N} \left( \frac{1}{1 + \tau/\tau_D} \right) + 1 \quad (2)$$

The equation only depends on the mean stay time of fluorophores in the detection volume  $\tau_D$  and the mean number of observed fluorophores  $N$ . The autocorrelation function decays from zero time shift to long time shifts. For the time shift  $\tau_D$  the autocorrelation has decayed half this way. From  $\tau_D$  the diffusion constant can be calculated using

$$\tau_D = \frac{r_0^2}{4D} \quad (3)$$

The difference between start and the end value of  $G(\tau)$  is also called the contrast of the autocorrelation function. The contrast  $1/N$  is therefore related to the concentration and the effective detection volume  $V_{\text{eff}}$  by the relation  $c = N/V_{\text{eff}}$ .

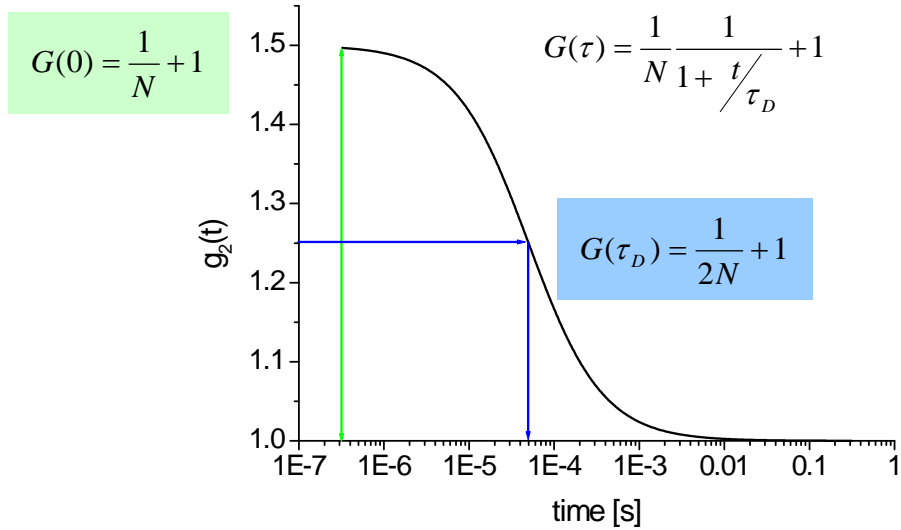


**Figure 2.2.** The (simplified) diffusional autocorrelation function  $G(\tau)$  in FCS.

In order to extract the interesting parameters from  $G(\tau)$  for single-component-systems, the more detailed model (3) can be assumed:

$$G(\tau) = 1 + \frac{1}{N(1 + \tau/\tau_D)} \left(1 + r^2 \tau/\tau_D\right)^{-\frac{1}{2}} \quad (4)$$

denotes the characteristic diffusion time, which is given by the radial  $1/e^2$ -Radius of the molecule detection efficiency assumed as Gaussian ellipsoid with two equal radial axes  $w_0$  and the diffusion constant  $D$ . The so-called shape factor  $r$  describes the ratio of axial to radial  $1/e^2$  radius.

$$r = \frac{z_0}{r_0} \quad (5)$$

The number of diffusing units in the detection volume is  $N$ . The detection volume can be calculated with the following formula [P. Schwille and E. Haustein, 2002]:

$$V_{eff} = \pi^{3/2} r_0^2 z_0 = \frac{N}{c} \quad (6)$$

If the concentration  $c = N/V_{eff}$  and  $D$  are known,  $z_0$  and  $w_0$  can be determined. If  $z_0$  and  $w_0$  are known,  $c$  and  $D$  can be determined.

In reality, the autocorrelation function is reduced by a factor of  $\left(1 - \frac{I_b}{I_{tot}}\right)^2$ , where  $I_b$  is the intensity of an uncorrelated background signal, which should be determined separately and  $I_{tot}$  is the total measurement intensity.

In case of high intensities, the triplet state becomes increasingly populated and therefore the autocorrelation function can be modified using the empirical parameters  $T$  and  $\tau_T$ , which are complex functions of the triplet kinetics.

$$G_t(\tau) = \left(1 + \frac{T e^{-\tau/\tau_T}}{1-T}\right) \quad (7)$$

### 3.3. Devices

The experiments will be conducted using the principle scheme (Figure 2.3) of fluorescence microscopy.

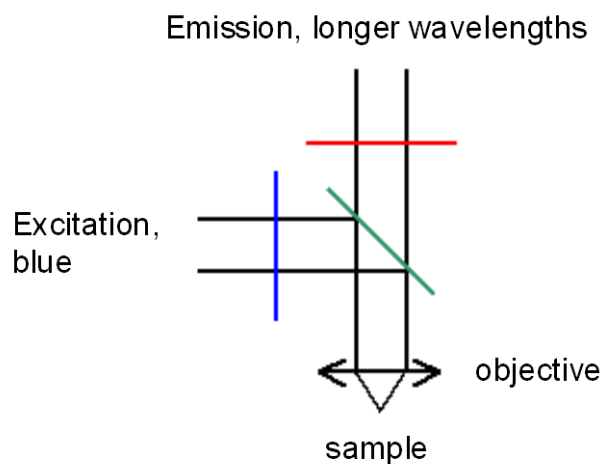


**Figure 2.3.** Confocal Fluorescence Microscopy using an infinity-corrected objective. Blue: Shortpass filter (or no filter when using a laser). Red: long-pass filter. Green: Dichroic mirror.

For excitation of the fluorescence an argon ion laser (488 nm wavelength) can be used. The fluorescence light is detected using an Avalanche Photo Diode (APD). The beam diameter of the excitation light is enlarged using two lenses. Here it is important, that the distance between these two lenses is such, that the beam remains parallel in order to ensure a good z-resolution. Between these lenses spatial filtering can be performed using pinholes. The emission light is focused onto a small detector area in order to get high resolution. An example of a detailed set-up is depicted in Fig. 2.4.

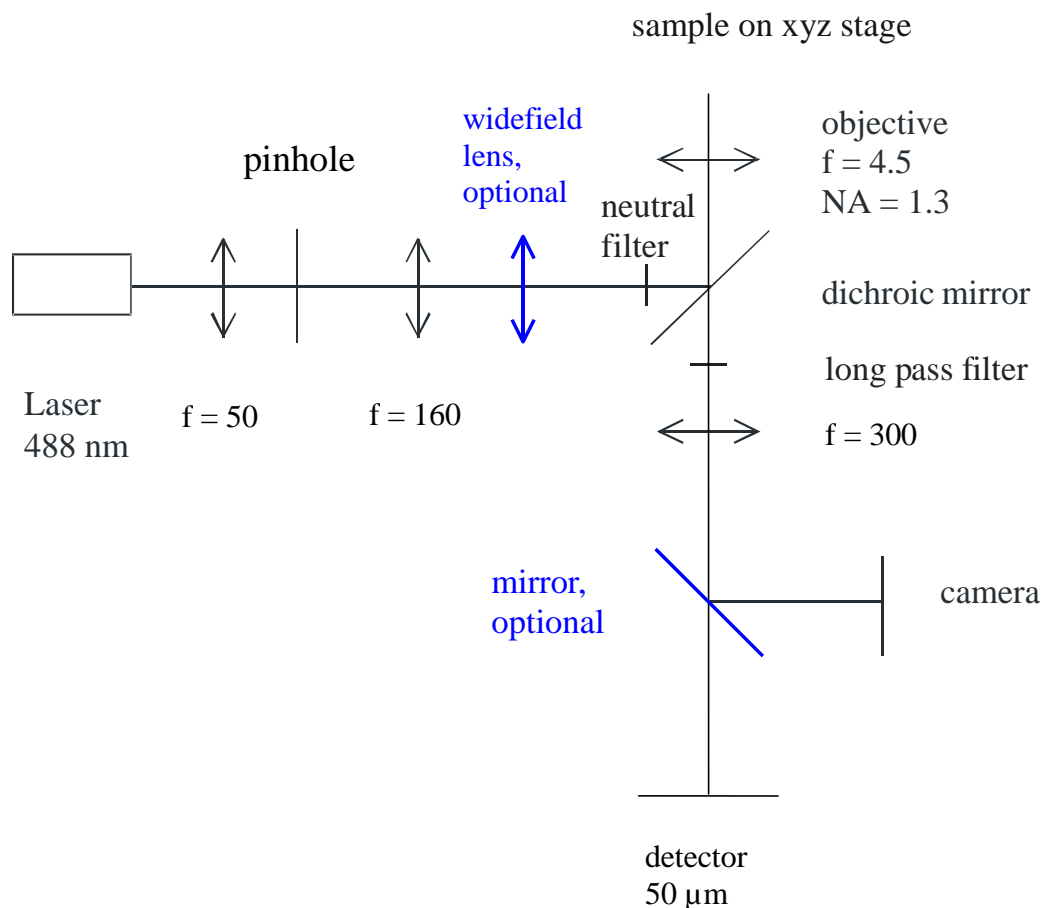


**Figure 2.4.** Set-up for confocal fluorescence correlation spectroscopy and for widefield microscopy. The focal lengths of the lenses are given in mm. The xyz stage can be moved using piezo actuators. By using the blue elements the set-up turns into a conventional (wide-field) microscope.

### 3.4. Materials

The dye Rhodamine 6G will be used for calibration of the observation volume. It will be used as an aqueous solution whose concentration will be determined using UV spectroscopy.

The micelle solution should be used in a concentration of less than 0.1 mg/ml.

### 3.5. Safety precautions

When working with the laser, never look into a reflection or the beam itself. When using the 100 mW laser you should wear safety goggles.

**IT IS NOT ALLOWED TO WEAR WATCHES OR RINGS.**

**DO NOT BEND OVER THE SET-UP.**

**NEVER WORK ALONE IN THE CHEMICAL LABORATORY.**

**DO NOT PUT ANYTHING IN YOUR MOUTH.**

### 3.6. Adjustment of the Set-up

(i) The sample can be applied onto a clean cover glass. Then adjust the height of the sample table to maximum intensity or check for the reflection from the upper surface of the cover glass.

(ii) Then raise sample the table by minimum 45  $\mu\text{m}$ .

(iii) Now you can adjust the detector (APD) to maximum intensity. Finally the cover glass correction is adjusted to maximum intensity.

Now step (i) until step (iii) are repeated. The excitation intensity is reduced until there is negligible triplet population in the autocorrelation function. The data are stored as ASCII files and can subsequently be evaluated.

### 3.7. Experiments

For the determination of diffusion constants and concentrations of the labelled micelles the autocorrelation function of a Rhodamine 6G solution with known concentration and diffusion constant ( $4.0 \times 10^{-10} \text{ m}^2/\text{s}$ ) is measured. Here adsorption



effects will be taken into consideration. From a non-linear least squares fit to this autocorrelation function you can determine the parameters  $z_0$  and  $r_0$ .

With these values of  $z_0$  and  $r_0$  in turn the unknown diffusion constant and the unknown concentration of the labelled nanoparticles can be calculated from a nonlinear least squares fit to the autocorrelation function of the labelled nanoparticles.

As the hydrodynamic radii of the particles might be distributed, the real autocorrelation function is the sum of the diffusional decays for fixed radii. The relative weights for each radius are given by the respective squared intensities corresponding to the signal times  $1/N_i$  with a different number of particles  $N_i$  for each radius. This distribution can be determined using the CONTIN algorithm. Thereby a constant grid of  $D_i$  is assumed and the corresponding weights  $I_i^2/N_i = N_i\phi_i^2$  are varied until they fit the measured function. Here  $\phi_i$  would denote the brightness of the particles corresponding to the diffusion constant  $D_i$ , if there would be no distribution of brightnesses. If the observation volume is not perfectly Gaussian [see S. T. Hess and W. W. Webb, 2002], it can be fitted with a hyperbolic and an exponential function. Such a complex function can also be implemented in the CONTIN algorithm.

### 3.8 Experimental procedures

1. Preparation of the Micelles solution
  - 1.1 Take 100  $\mu\text{l}$  of stock solution and dissolve it in 900  $\mu\text{l}$  of millipore water. Use eppendorf for storing the solution.
  - 1.2 Take the solution into syringe and mount the filter (0.2  $\mu\text{m}$  poresize). Press the solution through the filter to another eppendorf.
2. Calibration of confocal volume
  - 2.1 Take the stock solution of R6G in water provided by supervisor (OD=0.88) on measured with 1 cm cuvette.  $\epsilon_0=100000 \text{ L}/(\text{mol cm})^{-1}$
  - 2.2 Calculate the approximate concentration according to Beer-Lamberts law.
  - 2.3 Measure the first prepared solution (set dwell time 1  $\mu\text{s}$ , 50 or 100 sweeps) all measurements should be repeated 4 times for statistics.

- 2.4 Dilute the solution 10 times and repeat the measurement (repeat procedure with 3 different dilutions, last dilution should be 1:1000)
- 2.5 Measure the FCS curve as the function of excitation power. Take the solution which has shown the best signal to noise ratio of the autocorrelation function curve. Start from power of  $40\mu\text{W}$  end power 1-2 mW. Countrate of the MPD should not exceed 1 million counts/s.

**Questions:** How the used concentration and excitation intensity influence the experimentally determined confocal volume and diffusion time.

### **3. Determination of the diffusion constants and the hydrodynamic radius of the micelles in water.**

- 3.1 Take the  $20\ \mu\text{l}$  of water and drop it to the coverslip and add  $5\ \mu\text{l}$  of filtered micelle solution. Wait ca 1-2 minutes. Set the laser excitation power to  $40\ \mu\text{W}$ , dwell time  $10\ \mu\text{s}$ . Measure the ACF curve (at least two times with two different concentrations and two different excitation intensities).

#### **3.9. Literature**

Z. Földes-Papp, U. Demel, W. Domej and G. P. Tilz; "A New Dimension for the Development of Fluorescence-Based Assays in Solution: From Physical Principles of FCS Detection to Biological Applications", *Exp. Biol. Med.* **227**, 291–300 (2002).

S. T. Hess and W. W. Webb; "Focal volume optics and experimental artifacts in confocal fluorescence correlation spectroscopy", *Biophys. J.* **83**, 2300-2317 (2002).

P. Schwille and E. Haustein; "Fluorescence correlation spectroscopy. An introduction to its concepts and applications"; <http://www.biophysics.org/education/schwille.pdf>, 2002.

H. Zettl, Y. Portnoy, M. Gottlob, G. Krausch; "Investigation of micelle formation by fluorescence correlation spectroscopy", *J. Phys. Chem. B* **109**, 13397-13402 (2005).

### **3. Atomic Force Microscopy (AFM)**

AIM: To determine the topography of films and to image the micelles

#### **3.1. Introduction**

This technique maps the topography of a surface and can analyse the surface structure of polymer films. These investigations are performed by scanning the sample with a sharp needle of silicon. For soft materials like polymers normally the TappingMode™ with an oscillating needle is used. During the scan the change of the oscillating frequency and the amplitude of the oscillation is measured. These changes are correlated to the topography of the sample and to the hardness of the respective material. You can find a detailed description of the technique in the attached review article.

General references:

- [1] Köhler, R.; Phasen- und Transportverhalten von Triacontansubmonolagen an der Grenzfläche zwischen Luft und Siliziumoxid/Silizium, PhD thesis, Max-Planck-Institut für Kolloid- und Grenzflächenforschung, Universität Potsdam (2007).
- [2] Takano, H.; Kenseth, J. R.; Wong, S. S.; OBrien, J. C.; Porter, M. D.; Chem. Rev. **99**, 2845 (1999).
- [3] H.-J. Butt, B. Cappella, M. Kappl; Surface Science Reports **59**, 1 (2005).

#### **3.2. Theory**

##### **3.2.1. The Technique**

Atomic Force Microscopy (AFM), known also as Scanning Force Microscopy (AFM), has been invented in 1986 by Binnig and co-workers [4]. The physical quantity that is measured with this apparatus is the force between a sharp conical tip and a sample surface while scanning the tip across the sample. This allows investigations to be performed on a wide range of materials including polymers. AFM probes the surface of a sample using a sharp tip, with a terminal radius often less than 10 nm. The tip is located at the free end of a cantilever (100 µm long) with an elastic modulus that can be as low as a few 0.1 N/m. Forces of a few pN between the

tip and the sample surface cause vertical deflections of the cantilever on the Ångström scale. A laser beam bounces off the back of the cantilever onto a position-sensitive detector (PSD). As the cantilever bends, the position of the laser beam on the detector shifts (Fig. 3.1). The PSD itself can measure displacements of light beams as small as 1 nm. The ratio of the path length between the cantilever and the detector to the length of the cantilever produces a mechanical amplification. As a result, the system can detect sub-Angstrom vertical movements of the cantilever tip. The measured cantilever deflections enable the computer to generate a map of the surface topography. The interaction forces in the AFM are often quite complex due to several factors:

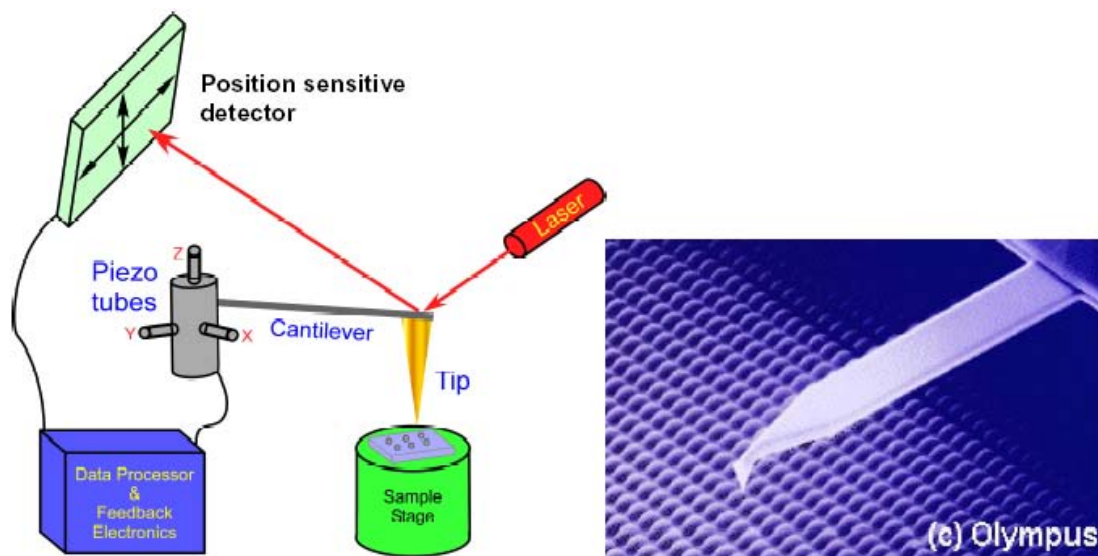


**Figure 3.1.** Principle of AFM (left), electron micrograph of a AFM cantilever above the sample surface (right).

- Even if the tip apex should be monoatomic, the number of atoms from the tip involved in the interaction is not only one, due to the contribution of rather long range forces;
- The forces are dependent on the environment (gas, liquid or vacuum);
- The scan is a dynamic process, which means that velocity dependent forces need to be considered;
- The tip can deform the sample.

A deep insight into this technique and results on organic and biological materials can be found in [2].

### **3.2.2. Forces in AFM**

It is important to distinguish the type of forces between the tip and the sample in order to separate the contributions and correctly interpret the experimental results [5].

#### **(i) Long Range Forces**

1. Van der Waals forces: they are due to atomic polarizability and therefore very general. They are proportional to  $1/r^6$  where  $r$  is the distance between them. The role of these forces in AFM has been discussed by Moiseev [6] and Hartmann [7]. They have a spatial extent that goes from one to tens of nm.

2. Electrostatic forces: they are due to coulomb interactions; in the present case they can occur between an electrostatically charged tip and a charged area of an insulating surface. They have a spatial extent that goes from one to thousands of Ångström.

3. Capillary forces: the curvature at the contact between the tip and the sample causes the condensation of vapor from the ambient including water from the air. Also surfaces exposed to the air environment are typically coated by a layer of water, whose thickness depends on the relative humidity (RH) of the atmosphere and on the physico-chemical nature of the object. Strong attractive capillary forces (about  $10^{-8}$  N) result, which hold the tip in contact with the surface. To avoid capillary forces the relative ambient humidity must be at RH=0%, although Thundat and co-workers demonstrated that below RH=10% they could not detect decays any further of the capillary forces [8]. Two simple experimental procedures can minimize the effect of this kind of forces: Firstly, working in a fluid cell with both tip and sample immersed in a liquid. Secondly, using a sealed chamber for the measurements filled with dry nitrogen for example [9].

#### **(ii) Short Range Forces**

1. *Repulsive forces*: The interatomic repulsion forces is due to electrostatic repulsion between nuclear charges. They are proportional to  $1/r^n$  with  $n>8$ .

2. *Forces of covalent bonds*: they originate from the overlap of the wave functions of two or more atoms. In this case the density of electronic charges is concentrated between the two nuclei. This force decreases abruptly for a separation over a few Ångström. The type of interaction can be also called *chemisorption*.

3. *Metallic adhesion*: they derive from the interaction between strongly delocalized electronic clouds, which cause strong interactions that decay exponentially with distance. They are important when two metallic surfaces approach to the extent that the electronic wave functions overlap [10]. This case can be called also physisorption.

4. *Friction*: during the scan, there is a force component parallel to the surface, since the tip is not always oriented exactly perpendicular to the surface. This friction tends to twist the cantilever, and since the torsion angle depends on the composition of the surface, the measurement of the twist provides chemical information [11]. It was also shown that this kind of friction force can be detected at the atomic scale [12]. As a first approximation, the forces contributing to the deflection of an AFM cantilever can be considered the *van der Waals* and the *interatomic repulsive forces*, which can be derived from the Lennard-Jones potential.

$$\varepsilon_r = -4\varepsilon_0 \left[ \left( \frac{\sigma}{r} \right)^6 - \left( \frac{\sigma}{r} \right)^{12} \right] \quad (1)$$

With:  $\varepsilon_0$  = potential energy at the minimum,  $s$  = effective molecular diameter,  $r$  = interatomic distance.

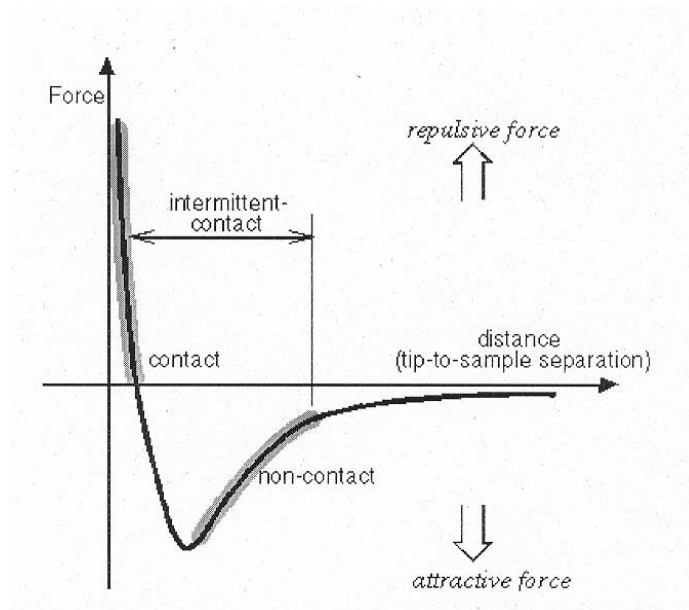


**Figure 3.2.** The Lennard-Jones potential in form of a force vs. distance curve with regions of contact, intermittent contact, non-contact mode.

The force is the negative gradient of the energy; it is plotted in figure 3.2. Two distance regimes are highlighted: 1) the contact regime; and 2) the non-contact regime. In the contact regime, the cantilever is held less than a few Ångströms from the sample surface, and the interatomic force between the cantilever and the sample is repulsive. In the non-contact regime, the cantilever is held on the order of tens to hundreds of Ångströms from the sample surface, and the interatomic force between the cantilever and sample is attractive (largely a result of the long-range van der Waals interactions). Both contact and non-contact imaging techniques are described in detail in the following sections.

### 3.2.3. Contact Mode AFM

In contact mode AFM a tip makes soft physical contact with the sample. The tip is attached to the end of a cantilever with a low spring constant, lower than the effective spring constant holding the atoms of the sample together. As the scanner gently scans the tip across the sample (or the sample under the tip), the contact force causes the cantilever to bend in order to follow the topographic profile. Using very stiff cantilevers it is possible to exert large forces on the sample and the sample surface is likely to get deformed; this may be also used in nanolithography. The total

force that the tip exerts on the sample is the sum of the capillary plus cantilever forces, and must be balanced by the repulsive and van der Waals forces for contact AFM. The magnitude of the total force exerted on the surface varies from  $10^{-8}$  N (with the cantilever pulling away from the sample almost as hard as the water is pulling down the tip), to the more typical operating range of  $10^{-7}$  to  $10^{-6}$  N. The contact mode AFM can generate the topographic data set by operating in one of two modes: Constant height or constant force mode. In constant height mode, the spatial variation of the cantilever deflection can be used directly to provide the topographic data set because the height of the scanner (consequently also the distance sample surface - tip holder) is fixed as it scans. In constant force mode, the deflection of the cantilever is used as input to a feedback loop that moves the scanner up and down in Z-direction, responding to the topography by keeping the cantilever deflection constant. In this case, the image is generated from the scanner's motion. With the cantilever deflection held constant, the total force applied to the sample is constant. In constant force mode, the speed of scanning is limited by the time of response of the feedback loop, but the total force exerted on the sample by the tip can be controlled. This mode is usually preferred for most applications because it gives a real topographic map of the sample surface. Constant height mode is often used for recording atomic-scale images of atomically flat surfaces, where the cantilever deflections and thus variations in applied force are small. This latter mode is also essential for monitoring fast processes in real-time, where high scan speed is essential.

#### **3.2.4. Non-Contact Mode AFM**

To overcome the problem of the friction component during scanning in contact mode, and to minimize the forces exerted from the tip on the sample and the effect of the capillary forces, alternative modes have been invented where the AFM cantilever vibrates near (on the order of tens to hundreds of Ångströms) the surface of a sample (figure 3.3). Basically, a stiff cantilever is forced to oscillate near its resonant frequency (typically from 200 to 400 kHz) with an amplitude of a few hundreds of Ångströms. While the tip scans over the sample the system detects the amplitude of the oscillation of the cantilever and keeps it constant with the aid of a feedback system that moves the scanner up and down. By keeping the amplitude constant, the system is expected to also keep the average tip-to-sample distance constant. The



sensitivity of this detection scheme provides sub-Ångström vertical resolution in the image, as in contact AFM. Due to the elimination of the shear forces that are applied from the tip to the sample, these modes are particularly useful for studying soft or elastic materials such as biological and organic films. As a consequence of the reduction of the overall interaction forces between the tip and the sample surface, these modes do not suffer from tip or sample degradation effects that are sometimes observed after taking numerous scans with contact AFM. Unfortunately, the lateral resolution that can be reached is a few nanometers, which is lower than in the contact mode.

**(i) Non-contact Mode**

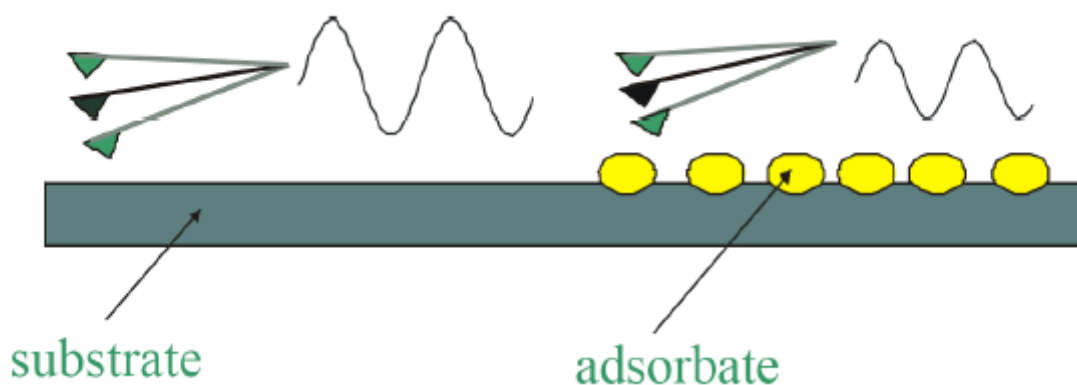


**Figure 3.3.** Vibrating modes: the tip-sample interaction damps the amplitude and shifts the phase of oscillation.

In this mode the tip-sample interaction is indicated on the force-distance curve of figure 2 as the non-contact regime. Since the force between the tip and the sample in this regime is low (generally about  $10^{-12}$  N), the force measurement is more difficult than in the contact regime, where it can be several orders of magnitude larger. Furthermore, cantilevers used for non contact mode must be stiffer than those used for contact AFM because soft cantilevers can be pulled into contact with the sample surface. The small force values in the non-contact regime and the greater stiffness of the cantilevers used for NC-AFM are therefore both factors that limit the force resolution, and consequently the lateral resolution, which can be achieved.

### **3.2.5. Tapping Mode**

Tapping Mode or intermittent-contact atomic force microscopy is similar to the non contact mode, except that for tapping mode the vibrating cantilever-tip is brought closer to the sample so that at the bottom of its travel it just barely hits, or taps the sample [13, 14, 15]. The intermittent-contact operating region is indicated on the curve in Figure 3.4. It notably increases the lateral resolution. In general, it has been found that TM-AFM is more effective than NC-AFM both for imaging larger scan sizes that may include greater variation in sample topography and for the slightly higher resolution that can be achieved due to the stronger tip-sample interaction forces that are sampled. Making use of the Phase Imaging mode, which operates detecting the shift in phase of the vibration, it possible to increase further the spatial resolution [16, 17]. In this imaging mode the contrast originates from differences in surface adhesion and viscoelasticity; it is therefore very helpful to detect different phases that coat the sample surface. The basic set-up of tapping mode AFM is shown in figure 3.4.

### **3.2.6. Piezoelectric Scanners and Scanning Artifacts**

Actuators (scanner) used in AFM are usually made of a single piezoceramic tube that is radially polarised. The tube is plated on the inside and on the outside with an electrode material (usually nickel). The outer electrode is divided along the tube axis into four equal segments (Fig. 3.5). The tube bends when a voltage is applied between one of the outer electrodes and the inner electrode, due to the piezoelectric transverse effect. When opposite segments (referred to as  $x$  and  $-x$  or  $y$  and  $-y$ ) are driven by a signal of the same magnitude but opposite sign, the tube is bent twice as much. The bending permits the probe or the sample to move in two dimensions (approximately on a sphere). The inner electrode is usually driven by the signal that adjusts the sample-probe-distance (usually referred to as  $z$ -direction).

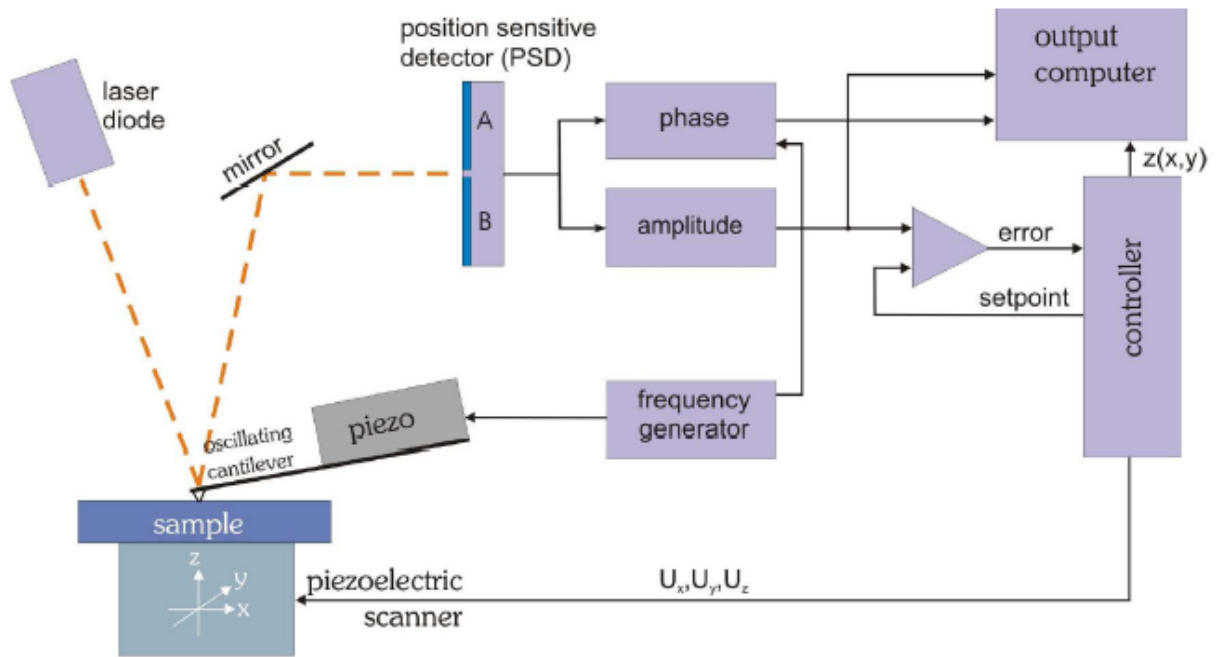


**Figure 3.4.** The setup for tapping mode AFM.

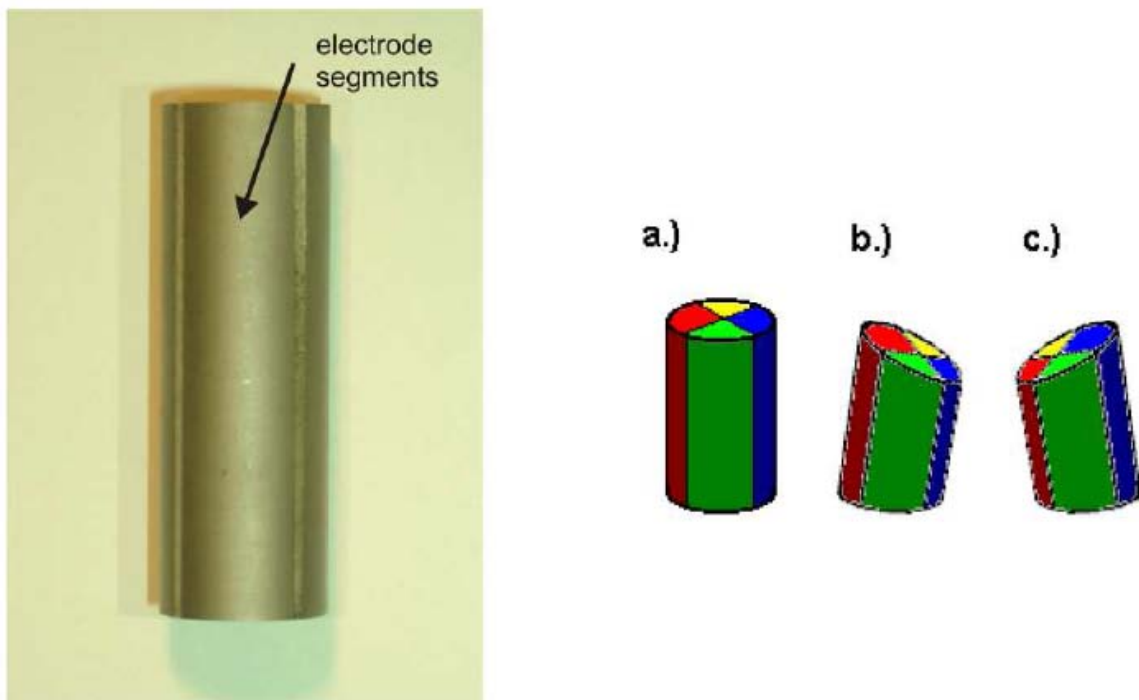


**Figure 3.5.** Piezoelectric scanner tube (left), scheme of the movement of a piezoelectric scanner tube.

The applied electric field,  $E$ , and the relative strain,  $S$ , (the relative deformation of a body) are related merely by the piezoelectric strain constant,  $d$ , when the actuator is allowed to freely deform (without mechanical stress).  $S = d E$ . Since  $d$  is

temperature dependent and not truly constant for large applied electric fields (e.g. large driving voltages) also the sensitivities for the x, y and z direction of a piezoelectric tube are not constant. Furthermore, the piezoelectric actuators follow a hysteresis curve and the displacement of an actuator is time dependent (creep). All these problems make it difficult to calibrate a piezoelectric tube and introduce scanning artifacts when the piezo is driven over large distances.

### **3.3. Sample Preparation**

The polymer films for the AFM experiments are prepared on cleaned silicon. For this purpose small pieces (1x1 cm<sup>2</sup>) of silicon are broken from the wafer. The pieces are first cleaned using a mixture of chloroform and acetone to remove organic impurities. After 10 min in the solution the silicon is cleaned with the SnowJet. With this procedure we obtain a clean and on the atomic level flat substrate for our polymer films. The polymer films are prepared by spin coating. Therefore the cleaned silicon is placed on the spin coater and a velocity of 2000 rpm is set. 30 - 40 µL of the polymer solution is placed on the silicon and the rotation is started. After 1 min the polymer film is prepared. Another possibility to prepare the sample is dip coating. In this case the silicon is dipped into the polymer solution for a few seconds and dried afterwards.

### **3.4. AFM Measurements**

The AFM measurements of the micellar solution give an approximation of the size of

the micelles. The phase contrast shows the variations in the materials and allows it to distinguish the different blocks of the polymer.

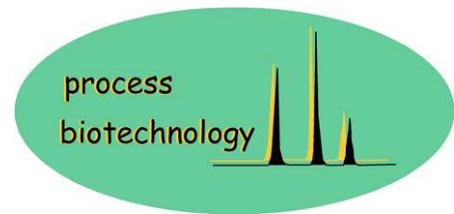
### **3.5. Literature**

[1] Köhler, R., Phasen- und Transportverhalten von Triacontansubmonolagen an der Grenzfläche zwischen Luft und Siliziumoxid/Silizium, PhD thesis, Max-Planck-Institut für Kolloid- und Grenzflächenforschung / Universität Potsdam, (2007).

- [2] Takano, H.; Kenseth, J. R.; Wong, S. S.; OBrien, J. C.; Porter, M. D. Chem. Rev. **99**, 2845 (1999).
- [3] H.-J. Butt, B. Cappella, M. Kappl, Surface Science Reports **59**, 1 (2005).
- [4] G. Binnig, C.F. Quate, C. Gerber, Phys. Rev. Lett. **56**, 930 (1986).
- [5] J. Israelachvili, Intermolecular and Surface Forces, (Academic Press, San Diego 1992).
- [6] Y.N. Moiseev , V. M. Mostepanenko, V. I. Panov, I Y. Sokolov, Phys. Lett. A **132**, 354 (1988).
- [7] U. Hartmann, Phys. Rev. B **42**, 1541 (1990). [8] T. Thundat, X. Y. Zheng, G. Y. Chen, R. J. Warmack, Surf. Sci. Lett. **294**, L939 (1993).
- [9] A. L. Weisenhorn, P. Maivald, H.-J. Butt, P. K. Hansma, Phys. Rev. B **45**, 11226 (1992).
- [10] A. Banerjea, J. R. Smith, J. Ferrante, J. Phys. Condens. Matt. **2**, 8841 (1990).
- [11] C. M. Mate, Phys. Rev. Lett. **68**, 3323 (1992).
- [12] C. M. Mate, G. M. McClelland, R. Erlandsson, S. Chiang, Phys. Rev. Lett. **59**, 1942 (1987).
- [13] Q. Zhong, D. Inniss, V. Elings, Surf. Sci. **290**, 688 (1993).
- [14] J. Tamayo, R. Garcia, Langmuir **12**, 4430 (1996).
- [15] C. Bustamante, D. Keller, Physics Today, December (1995), pp.32-38.
- [16] P. Leclere, R. Lazzaroni, J. L. Brdas, J. M. Yu, P. Dubois, R. Jerome, Langmuir **12**, 4317 (1996).
- [17] S. N. Magonov, V. Elings, M. H. Whangbo, Surf. Sci. **375**, L385 (1997).
- U. Hartmann, An elementary introduction to atomic force microscopy and related methods. <http://www.uni-saarland.de/fak7/hartmann/en/download/page2.htm>.



UNIVERSITÄT  
BAYREUTH



# **Nanocontainers uptake in mammalian cells: a practical course**

*Interdisciplinary Lab course (Elite study program  
macromolecular science)*

*LS Bioprozesstechnik*  
**Prof. Dr. Ruth Freitag**

**Assistants:**  
**Dr. Valérie Jérôme**

## **CONTENTS**

**1. Introduction**

**2. Essentials of laboratory safety and good laboratory practice  
(Sicherheitshinweise)**

**3. Course**

**4. Annexes**

***A1. Composition of RPMI 1640 medium***

***A2. Essentials of laboratory safety***

## 1. Introduction

Ansprechpartner:

**Frau Dr. Valérie Jérôme**

Universität Bayreuth

LS Bioprozesstechnik

Universitätsstrasse 30

95440 Bayreuth

☎: 0921 55 7372

@: valerie.jerome@uni-bayreuth.de

## 1. Praktikumsregeln

Folgende Bedingungen müssen erfüllt werden:

1. entsprechender Arbeitsschutz (**Kittel, Schutzbrille, feste geschlossene Schuhe**). Kittel und Schutzbrille sind am Lehrstuhl Pflicht und **werden nicht** vom Lehrstuhl gestellt. Studenten die diese Gegenstände nicht mitbringen dürfen an das Praktikum **nicht teilnehmen**.
2. Am Gentechnische Sicherheitsbelehrung teilgenommen haben.
3. pünktliches Erscheinen zum Praktikum

Jegliche Missachtung dieser Praktikumsregeln führen zum sofortigen Ausschluss aus dem Praktikum. Des Weiteren ist dem Studenten untersagt dieses Praktikum zu wiederholen.

## 2. Sicherheitshinweise

*(Siehe auch A2. Essentials of laboratory safety)*

Die Zellen, mit denen im Praktikum gearbeitet wird, sind **keine gentechnisch veränderten Organismen**. Es geht von diesen Zellen keine Gefahr für Mensch und Umwelt aus. Die Verwendung von chemischen Gefahrstoffen wurde minimiert. Einzelne Arbeiten dürfen **nur mit Schutzbrille, Kittel, Handschuhen und festen Schuhen** (keine Sandalen) durchgeführt werden. Einmalhandschuhe liegen in den Praktikumsräumen aus. **Die Entsorgung von flüssigen Abfällen in der Spüle ist untersagt!** Feste und flüssige Abfälle werden gesammelt und umweltgerecht entsorgt.

**Essen, trinken, rauchen, und schminken ist in den Praktikumsräumen untersagt!**

**Straßenkleidung und Taschen müssen in den Spind (FAN D; Untergeschoß gleich neben den Aufzug; 2 Euro Pfand) aufbewahrt werden.**

In den Praktikumsräumen brauchen Sie nur das Praktikumsskript, einen Taschenrechner, und einen Notizblock.



**Chemical hazards: Hazard symbols and labels**

**Indication of hazard:** Hazard symbol

**Hazard labels include:** Hazard identification and code letter

**Original labels of bottles containing hazardous chemicals:**

- a) R-Phrases: indication of special hazards
  - b) S-Phrases: safety guidelines
- Code letter: hazard declaration of the substance












**Hazard labels**

([www.vis-technik.bayern.de/de/left/fachinformationen/chemie\\_basis/gefahrensymbole.htm](http://www.vis-technik.bayern.de/de/left/fachinformationen/chemie_basis/gefahrensymbole.htm) in German only!) (General information: <http://userpage.chemie.fu-berlin.de/~tlehmann/guidel.html#kapitelfuenf>)

The most prominent parts of the hazard labels of dangerous substances and preparations are the black pictograms on a yellow/orange background. You may have already noticed the “flammable” label on product of every-day life, e.g., hairspray, indicating the fuel gas included in this product. The absence of such label does not mean that this product confers no risk. Please read all security advices on the labels carefully. No hazard label for flammable substances with a flash point below 55°C exists, but is only declared with the phrase “flammable”. At elevated room temperatures such products may pose an equal danger potential as substances with the hazard label “highly flammable”. Also, substances dangerous at high concentrations, but present only at minor concentrations, may be indicated on the label of the container, e.g., sensitizing substances. These minor concentrations must not be declared but are of great importance to the worker, as they may cause allergies.

**What is the exact meaning of the hazard symbols?**

Study the pictographs concerning conformity and differences, and memorize the according code letters.

label	code letter	label	code letter
	E explosive		T toxic
	O oxidizing		Xn harmful
	F+ highly flammable		C corrosive
	F flammable		Xi irritating
No hazard label and code letter exist for “flammable” (flash point 21 - 55°C)	flammable		N dangerous for the environment
	T+ highly toxic		Special label for preparations and products containing asbestos according to <a href="#">GefStoffV</a>

**Why does no hazard label exist for „carcinogen“?**

No hazard labels exist for several dangerous properties. For example, “sensibilizing” substances are branded with the code letters X<sub>i</sub> (irritant) or X<sub>n</sub> (harmful). The following hazards lack a label as well: carcinogen, mutagen and teratogen. According to the power of the hazard the code letters T (toxic) or X<sub>n</sub> (harmful) are used. The special label for preparations and products containing asbestos is strictly speaking no hazard label according to the hazard regulation.

# Introduction to Mammalian Cell Culture

Assistant: Dr. Valérie Jérôme

## 1. Experimental Aims

This practical course covers some basic manipulations typical for mammalian cell culture: work under sterile conditions in a laminar flow hood and enzymatic detachment of cells from substrates. Further on, the flow cytometry method will be used to perform a quantitative analysis of nanocontainers uptake, making use of fluorescent dyes.

## 2. Materials and Methods

### 2. 1. Cell Line

The CHO is a permanent cell line derived from Chinese hamster ovary. CHO cells are cultivated in attached monolayers (fig. 1). These cells adhere strongly to the cell culture dish. Therefore, a purely mechanical detachment will not work and the enzymatic treatment by trypsin is required to detach these cells from the plastic.

ATCC Number: **CCL-61**  
Designation: **CHO-K1**

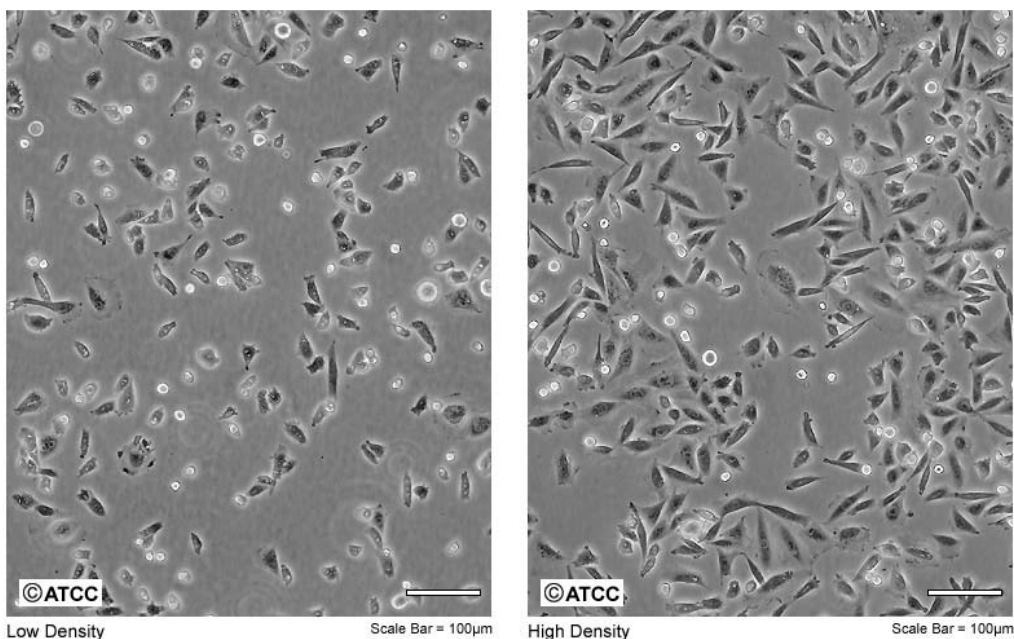


Fig 1: CHO cells at two different culture densities

## 2.2 Fluorochrome

### 2. 2. 1 Perylene

**Perylene** or **perilene** is a polycyclic aromatic hydrocarbon with chemical formula  $C_{20}H_{12}$ . The chemical structure of Perylene is shown in figure 2a. It has an absorption maximum at 434 nm, and as with all polycyclic aromatic compounds, low water solubility ( $1.2 \times 10^{-5}$  mmol/l) (<http://en.wikipedia.org>).

The perylene derivative (N,N'-Di(1-heptyloctyl)-perylene-3,4:9,10-tetracarboxylic diimide) used in this practical course has an absorption maximum at 526 nm and exhibits two emission peaks after excitation at 488 nm, one peak at  $\sim 530$  nm and one peak at  $\sim 625$  nm, for the monomer and an aggregated form, respectively. It was synthesized in the group of Prof. M. Thelakkat.

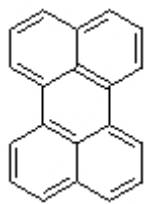


**Fig. 2a:** Perylene

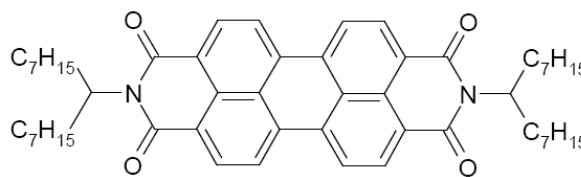


**Fig. 2b:** Perylene bisimide (PBI) derivate

### 2. 3. Cultivation

Cells are cultivated in the standard medium, RPMI 1640 medium (see annex 1 for complete medium formulation). The medium is supplemented with:

- 10% Fetal Calf Serum (FCS)
- 2 mM L-glutamine

**Table 1: Quantity of medium to be used for different plate size**

Tissue culture plate type	Filling volume (ml)
10 cm tissue culture plate	10
6-well plate	2-3 per well

For this practical course, cells are grown in CO<sub>2</sub> incubator (5% CO<sub>2</sub>, 95 % humidity and 37°C).

### 2. 4. Microscopy

Before starting any work with your cultures, you will have to observe yours cultures carefully and determine their status and health. Examine the medium in the vessel for macroscopic evidence of microbial contamination. This includes unusual pH shifts (yellow or purple color from the phenol red), turbidity or particles. Also, look for small fungal colonies that float at the medium-air interface. Then, with an inverted microscope, check the medium for evidence of microbial contamination (fig. 3) as well as the morphology of the cells (fig. 1). Bacteria contamination will appear as small, shimmering black dots within the spaces between the cells. Yeast contamination will appear as rounded or budding particles, while fungi will have thin filamentous mycelia. Most adherent cells should be attached firmly to the surface. In some case, healthy cells will round up and detach somewhat during mitosis and appear very refractive. Following mitosis, they will reattach. In contrast, dead cells, often round up and detach from the monolayer and appears smaller and darker (not refractive) than healthy cells. During this practical course, you will use a conventional inverted microscope (Olympus CKX41).

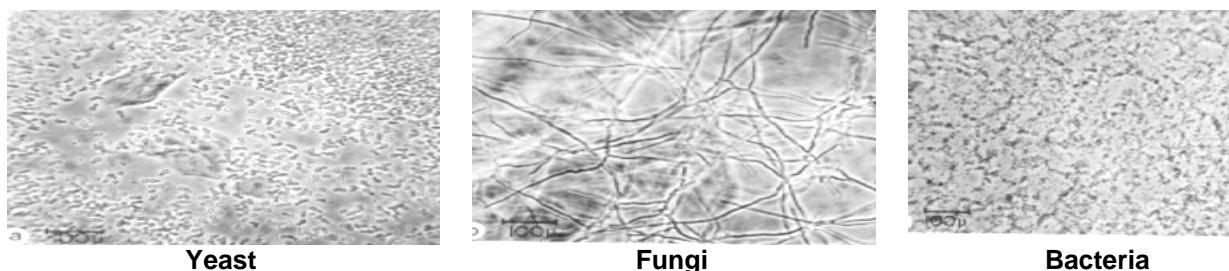


**Fig. 3:** Microbial contaminations

## 2. 5. General Handling

### 2. 5. 1. Harvesting adherent cells

All the following cell manipulation must be done work under sterile conditions in a laminar flow hood

1. The culture medium is removed using a sterile Pasteur pipette connected to a siphon-like recipient coupled to a vacuum pump.
2. The cells are washed twice with 2ml PBS 1X (Phosphate-buffered saline) to remove traces of serum (serum inactivate the enzymatic effect of the trypsin).
3. Trypsin/EDTA is added: **0.5ml/ well** for a 6-well plate. Cells are rinsed with the trypsin/EDTA solution. The excess of trypsin/EDTA is removed. The cells are exposed to trypsin/EDTA at room temperature until they detach, usually 2 to 4 minutes. If the cells do not detach properly the trypsinization can be carried out at 37°C to accelerate the digestion of proteins responsible for adhesion onto to the plastic surface of the flask. Weakly attached cells can alternatively be detached by hitting the culture plates on the workbench.
4. Enzymatically detached cells are resuspended in serum containing medium to inactivate the trypsin, in 1ml of fresh medium.
5. The cell suspension in the culture plate is pipetted gently up and down several times in order to separate aggregated cells (**Try to avoid air bubbles**). Now the single cell suspension can be transferred into a 15 ml Falcon™ tube. **Place on ice!**

**Cell washing in Falcon™ tube:** After centrifugation (§ 2. 5. 2.), discard the supernatant and resuspend the cell pellet in 5ml PBS 1X. Centrifuge and repeat the procedure at least once. This washing step removed all trace of serum components.

### 2. 5. 2. Centrifugation of cells

Cells are centrifuged at 200g for 5 minutes at 4°C (1000 rpm in a Heraeus Multifuge 3-SR).

## 3. Experimental protocol

During this practical course you will learn: (1) to work with animal cells under sterile condition in a biosafety cabinet; (2) to collect the cells and prepare them for the flow cytometry analysis.

### 3. 1. Materials

You will be provided with:

- RPMI 1640 – 10% FCS
- PBS 1X
- Trypsin/EDTA

You will be provided with two 6-well plates containing CHO cells plated the day before at the density  $2 \times 10^5$  cells/well. You will find all pipettes and small materials you needed in the practical course room.

### 3. 2. Analysis of block micellar nanocontainers up take by CHO-K1 cells

#### 3. 2. Incubation of the cells with the micellar nanocontainers

1. Sterile filter the micelles solution with a disposable membrane filter (Acrodisc syringe filter; 0.2 µm Supor Membrane, low protein binding, #PN4612).
2. Change the cell culture in each 6-well plate (two plates) by exchanging the “old medium” with 2 ml/well “fresh medium”.

3. Add the micelles solution in each well (see fig. 4). **When the volume to be added is > 200  $\mu$ l, first remove the corresponding medium volume before adding the micelles solutions.**
4. Place back the two plates in the CO<sub>2</sub> incubator for the next 16 to 24h.

No micelle	Quantity 1 micelles	Quantity 2 micelles
Quantity 3 micelles	Quantity 4 micelles	Quantity 5 micelles

**Fig. 4:** Quantity of micelles solution to be added in the 6-well plates.

### 3. 2. 2 Analysis of the nanocontainers uptake with flow cytometry

After 16 - 24h incubation of the CHO-K1 cells with the micelles, the medium will be removed, the cells washed twice with 3 ml PBS1X and collected by trypsinization as described in § 2. 5. 1. The cell suspension will be washed once with 1ml RPMI-10% FCS. The cell pellet will be then resuspended in 0.5 to 1 ml PBS1X (depending on the pellet size).

The samples will be then analyzed with a flow cytometer (Cytomics FC500; Beckman Coulter) using the 488nm laser (see fig. 5 for optical system scheme). The size and granularity of the cells will be detected in FSC (forward scatter) and SSC (side scatter), respectively. The perylene fluorescence will be detected in FL1 (monomer) and FL3 (aggregated form)(fig. 6).

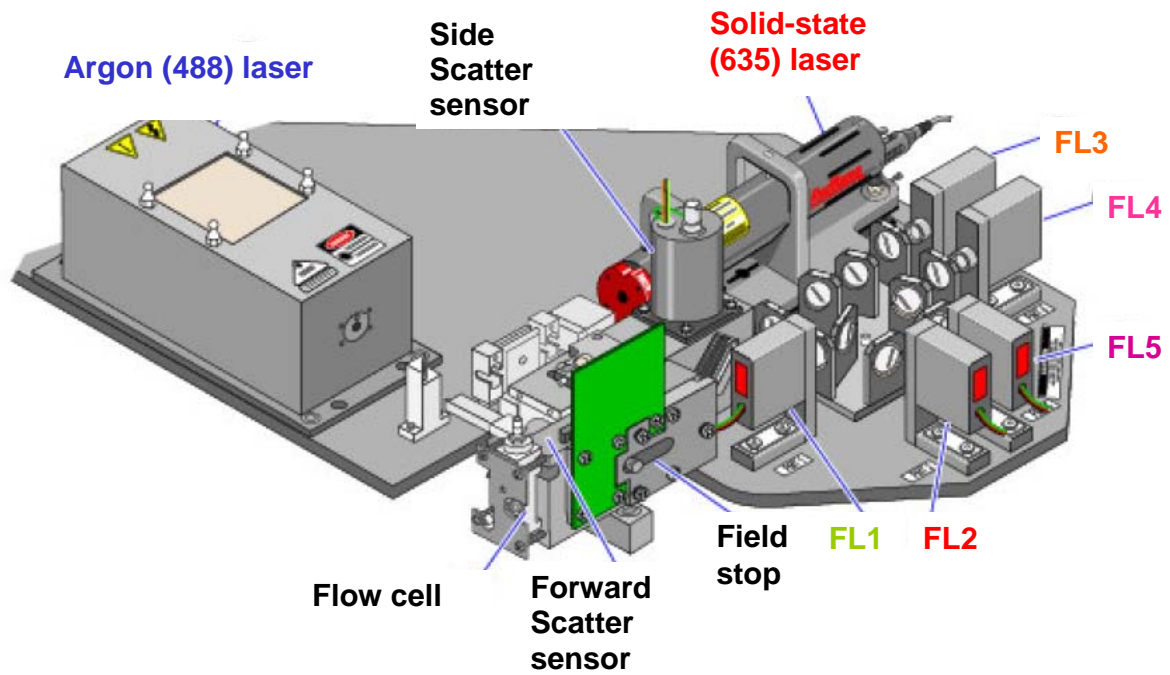


Fig. 5: Flow cytometer optical system

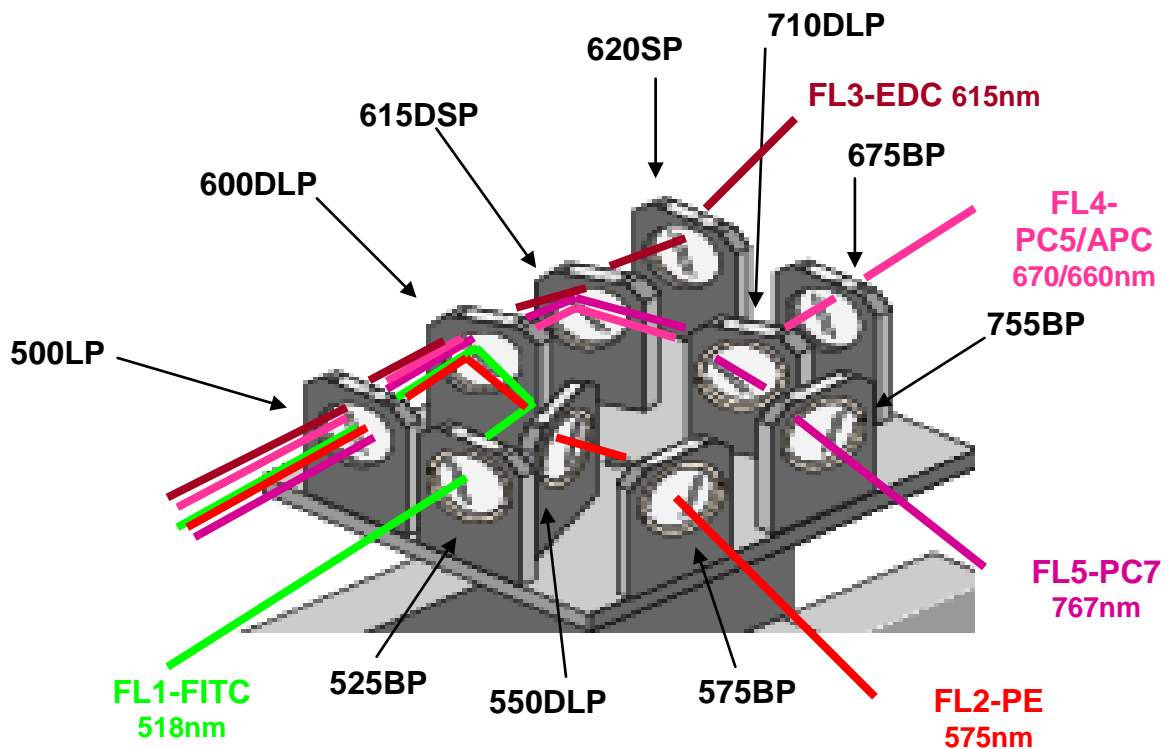


Fig. 6: Filters used for spectral separation

**References:**

Freshney, R. (1987) Culture of Animal Cells: A Manual of Basic Technique, p. 117, Alan R. Liss, Inc. Dr. J. Paul Robinson <http://www.cyto.purdue.edu/flowcyt/educate/pptslide.htm>

Nunez, R. (2001). Introduction to the field of cytometry and its importance in biomedicine. Curr. Issues Mol. Biol., 3 (2): 37-38.

## Annexes

### A1. Composition of RPMI 1640 medium (PAA; E15-039)

Formulation	mg/l
<b>Inorganic Salts</b>	
Calcium Nitrate · 4H <sub>2</sub> O	100.00
Potassium Chloride	400.00
Magnesium Sulphate dried	48.80
Sodium Chloride	6000.00
di-Sodium Hydrogen Phosphate	800.00
Sodium Hydrogen Carbonate	2000.00
<b>Amino Acids</b>	
L-Arginine · HCl	241.86
L-Asparagine · H <sub>2</sub> O	50.00
L-Aspartic Acid	20.00
L-Cystine	50.00
L-Glutamic Acid	20.00
Glycine	10.00
L-Histidine base	15.00
L-Hydroxyproline	20.00
L-Isoleucine	50.00
L-Leucine	50.00
L-Lysine · HCl	40.00
L-Methionine	15.00
L-Phenylalanine	15.00
L-Proline	20.00
L-Serine	30.00
L-Threonine	20.00
L-Tryptophan	5.00
L-Tyrosine	20.00
L-Valine	20.00
<b>Vitamins</b>	
D-(+)-Biotin	0.20
D-Calcium Pantothenate	0.25
Cholin Chloride	3.00
Folic Acid	1.00
myo-Inositol	35.00
Nicotinamide	1.00
p-Aminobenzoic Acid	1.00
Pyridoxine · HCl	1.00
Riboflavin	0.20
Thiamine · HCl	1.00
Vitamin B <sub>12</sub>	0.005
<b>Other Components</b>	
D-Glucose anhydrous	2000.00
Glutathione (red.)	1.00
L-Glutamine in E15-840, E15-842, E15-848	300.00
HEPES in E15-041 and E15-842	5958.00
Phenol Red in E15-039, E15-840, E15-041, E15-842	5.00

Literature: Moore, G. E., Gerner R. E. and Franklin, H. A. (1967) Culture of Normal Human Leucocytes. JAMA 199, 519-524

## A2. ESSENTIALS OF LABORATORY SAFETY



### Before Lab Work, Get to Know:

- Hazards of materials & agents and their prescribed safety procedures
- Emergency spill procedures, use of adsorbents and disinfectants
- Designated escape route and alternative
- Location of fire ext., eye wash, shower, first aid and spill kits
- Emergency telephone numbers and reporting procedures
- For emergencies call:



(9) 19222 for  
injured person



(9) 112 for fire





## While Working in the Lab:

- Shoes with full coverage and good grip soles
- Restrain long hair, loose clothing and jewelry
- Put always your lab coat on
- Use appropriate eye, skin and hand protection



### Eye protection

- Protects against risk of flying objects or dust particles, splashes of hazardous materials or harmful rays



### Hand protection

- Protects against risk of cuts, abrasions, burns, or exposure to hazardous material
- Requires selection of the appropriate chemical resistant gloves
- Use universal transfer devices  
Handle unknowns as if they were hazardous



- Handle volatiles in a chemical fume hood
- Handle biological materials in a biological safety cabinet



- Authorized persons only
- Identify EVERYTHING!
- No food, beverages, tobacco products, or application of cosmetics
- Report all accidents, injuries, fires, spills



### Before Leaving the Lab:

- Turn off:
  - Gas
  - Water
  - Power supplies
  - Vacuum lines
  - Compression lines
  - Heating apparatus
- Identify and package waste, dispose properly
- Decontaminate work surfaces and equipment
- Return unused equipment, apparatus, ...
- Leave lab coat in the lab
- Wash hands
- Close and lock door

